Augmented reality system for MRI-guided interventions: a cadaver study

Lam V.[1], Yarmolenko P. [1], Rajan P. [2], Hossbach M. [2], Demir A. [2], Foroughi P. [2], Cleary K. [1], Vellody R. [1], Sharma K. [1]
[1]Children's National Hospital, Sheikh Zayed Institute for Pediatric Surgical Innovation, 111 Michigan Ave NW, Washington, DC 20010, United States
[2]Clear Guide Medical Inc., 3600 Clipper Mill Rd Suite 400, Baltimore, MD 21211, United States

1. Abstract

Implementation of MRI guidance in place of CT or X-ray would reduce ionizing radiation exposure and provide better soft tissue contrast in a wide range of musculoskeletal targets in children. We developed an augmented reality guidance system for MRI-guided interventions. The purpose of this study was to evaluate the feasibility of using this system to target shoulder, hip, sacroiliac joints and liver in a cadaver.

The LUMENA AR system is designed to operate in an interventional MRI suite. Specially designed fiducial markers placed on the skin surface and needle hub are used to track needle position in real-time during advancement. T1-weighted images acquired after fiducial placement allow interventional radiologists to plan optimal needle paths to selected targets by choosing skin entry and target points on an in-room planning console. Two interventional radiologists placed 12 needles along planned trajectories by following the guidance plan projected onto the skin by the optical head. Each MRI scan required approximately 2 min, and each insertion was completed within 1 minute. "User error" was defined as the distance between final needle tip location and selected target after insertion. "Overall error" was calculated as the distance between the selected target and post-insertion MRI-derived needle tip locations. All errors were reported as average ± standard deviation across all locations.

Overall, 12 locations were targeted (3 shoulder, 4 hip, 1 liver, and 4 SI joint). The system operated as expected and all needles were placed successfully. User error was 2.4±1.1 mm (range: 0.8 – 4.2 mm). Overall targeting error was 2.6±0.6 mm (range: 1.5 – 3.6 mm).

The study demonstrates feasibility of using augmented reality to place needles under MRI guidance in a cadaver. The system was subjectively judged to be easy to use and to fit within the established clinical workflow of image-guided needle-based interventions.

Keywords

1 image-guided therapy
2 augmented reality
3 interventional radiology
4 percutaneous
5 MRI interventions

2. Introduction

Pediatric patients often present with non-specific symptoms of pain or reluctance to use the affected limb, or inability or bear weight. In these cases, prompt diagnosis and appropriate treatment

are essential. Tissue diagnosis is commonly obtained through image-guided needle-biopsy performed under ultrasound (US), computed tomography (CT) or X-ray imaging for guidance. However, some tissue targets are difficult to visualize with these imaging modalities and are better visualized with magnetic resonance imaging (MRI), which provides superior soft tissue contrast and similar spatial resolution compared to CT and US [1]. This is especially true for some musculoskeletal pathologies. After appropriate diagnosis, image-guided needle injections can also be used for precise local treatments such as injection of pain medications and/or steroids into a painful joint.

Prior reports have demonstrated the safety and feasibility of MR guidance for biopsies, spine procedures, cyst aspirations, therapeutic injections, and tumor ablation [2]. The use of CT and X-ray imaging exposes patients and interventionalists to ionizing radiation. In pediatric patients, there is a documented need to reduce such exposure, which is known to increase cancer incidence in children [3]. Therefore, MRI guidance of interventional procedures would be preferred, especially in young children. However, the MRI environment is highly restrictive, requiring special equipment and guidance tools that are deemed MRI-safe and/or compatible.

Several approaches that enable MRI-guided interventions have been proposed. Available optical and electromagnetic needle tracking technologies are difficult to adapt to the MRI environment [4], whereas MRI-compatible robotic guidance systems require a high degree of procedure-dependent customization and complexity [5]. Outside of the MRI suite, augmented reality approaches have been demonstrated [6, 7]. Such systems provide guidance using mirrors and projectors requiring complex calibration procedures and ample room in the interventional MRI suite [8, 9]. Unlike these projector-based approaches, AR headsets do enable fusion of guidance information and visualization of the target area. However, there are currently no MRI compatible AR headsets commercially available. MRI-guided interventions are time-consuming and involve multistep workflows. These employ either an in-bore needle advance, which has ergonomic and imaging sequence imitations, or an “advance and check” method, which interleaves incremental advancement of the needle with MR imaging [10]. These multistep, time-consuming processes could be shortened and simplified if an accurate and precise guidance system were designed for the MRI environment.

To address multiple existing limitations of commonly used MRI-guided intervention methods, we have developed an AR-based real-time guidance system designed to work continuously in the interventional MRI suite, enabling an improved clinical workflow [11]. The system allows radiologists to select the target, skin entry point, to plan the optimal needle path and to view this path on different imaging planes. The AR-based system also assists the radiologists during needle advancement to approach the target along the planned trajectory without having to scan multiple times as would be needed for the ‘advance and check’ method. In our previous study, we evaluated feasibility and accuracy of this system in custom-built shoulder phantoms [11]. To address clinical considerations prior to a clinical trial, the system’s performance was evaluated in a cadaver. The cadaver provides a realistic assessment as it better reproduces tissue heterogeneity, tactile feedback, and MRI characteristics of patients. The purpose of this study was to evaluate feasibility and performance of this system in MR-guided needle-based interventions to target hip, shoulder, and SI joints as well as liver targets in a human cadaver. The results provide additional confidence and help inform our clinical trial design.

3. Materials and Methods

The following sections describe hardware and software components of the LUMENA AR system (Clear Guide Medical Inc., Baltimore, MD, USA) as well as the workflow and data analysis methods used in the study.

Hardware components and MRI markers (VisiMARKERs)

The LUMENA AR system consists of a "CORE" panel PC and an optical head mounted on an MR safe mobile cart. Both panel PC and optical head (which included a stereo camera setup and a projector) were designed, developed, and fabricated for operating continuously beyond the 300 Gauss line. The aluminum mobile cart was used to safely mount the "CORE" PC, power adapter, and the articulated arm with the optical head device (Figure 1). During the procedure, the optical head is located above the patient and aimed at the target area.

Figure 1. Augmented reality LUMENA system for MRI-guided needle-based interventions. A panel PC and an articulated arm with an optical head mounted on an MR-safe cart. The system is designated MR conditional and designed for continuous operation in the MRI environment (<300 Gauss for the optical head and <100 Gauss for panel PC).

The fiducials used by the LUMENA system (VisiMARKERs) were designed and tested to be MR safe, sterilizable, and biocompatible for application on skin (Figure 2 Left). A pair of markers were attached onto an MRI-compatible needle to create a TipTAG needle that will be automatically tracked by the system (Figure 2 Right). MRI visibility was achieved using synthetic gel encapsulated inside the acrylic body of the marker and visible on T1-weighted and T2-weighted MRI scans.

Figure 2. Fiducial Markers. *Left:* VisiMARKER fiducials that are visible under both MRI and the optical head cameras. These allow the system to register the optically tracked target area to the MRI volume. *Right:* TipTAG needle. The tags are affixed to the needle and calibrated prior to the procedure for real-time tracking of the needle tip during intervention.

Software components: needle tracking, user interface for planning, navigation and projected feedback

Detection of MRI fiducials and communication between the camera system, the CORE computer and the projector were implemented as described previously [11]. The interface allows user to browse the MRI volumes, go through all the slices with options to zoom, and to adjust brightness and contrast while choosing entry and target points (Figure 3). The skin needle entry point selected by the user is projected as a small red circle on the skin surface. A pseudo-shadow of the needle assists with orientation prior to insertion and when advancing towards the target. As with a real shadow, the user orients the needle away from the projected line to minimize the shadow's length.

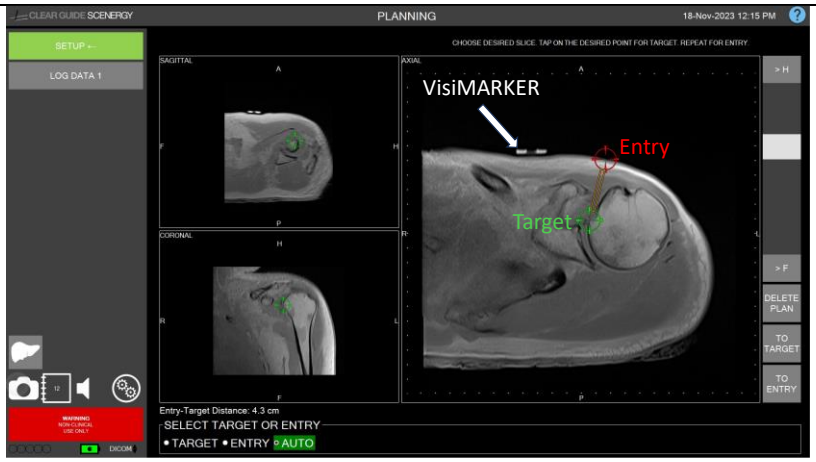

Figure 3. The Planning Interface. The 3 panes display axial, coronal and sagittal slices. The multi-slice planning interface allows the user to select target and entry points on either a single slice or separate slices. The system allows users visualize the path of the needle trajectory using the up and down scroll buttons. The selected target remains displayed as a green reticle on all 3 views. The distance from skin entry point to target is reported on the bottom left of the interface.

The distance between the needle tip and the target in millimeters is displayed in real-time on the patient's skin as a numerical indicator, and as a green circle which shrinks as the needle

approaches the target (Figure 4). This dynamic information is duplicated in multiplanar format on the CORE computer's monitor throughout the procedure.

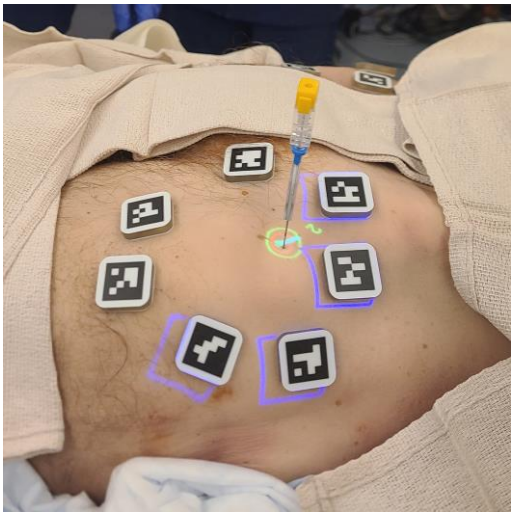

Figure 4. Projected guidance during needle insertion. The system projects a continuously updated set of guidance cues onto the skin around the target area, including the entry point, distance to target, and the needle's pseudo shadow (cyan line).

The MRI volume is resliced along the needle trajectory such that the full needle path plus the entry and target points are visible on a single slice; the intervention pane also displays the two planes perpendicular to the needle trajectory. The planned anatomical target remains visible on all 3 MRI slice views during intervention (Figure 5).

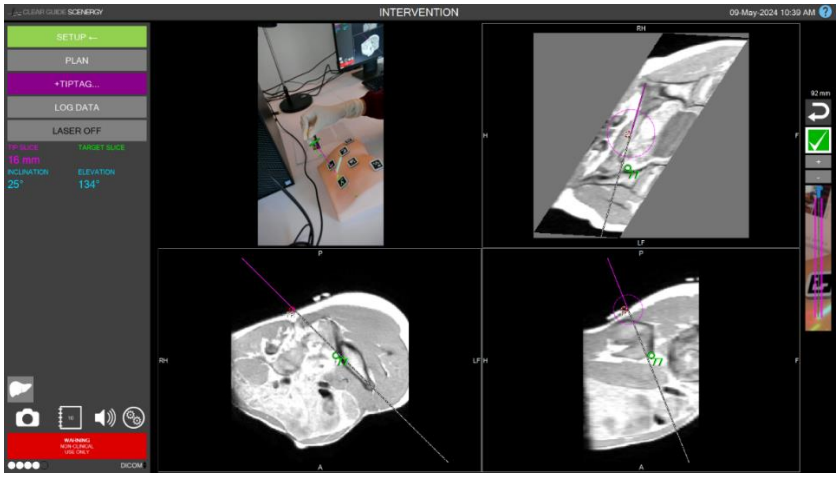

Figure 5. The Intervention Pane. *Top Left:* the live feed from the optical head camera. *Bottom Left:* the MRI volume has been resliced along the needle trajectory such that the full needle path, as well as entry and target points are visible on a single slice. *Top and Bottom Right:* the two planes perpendicular to the needle trajectory. The planned target remains visible on all 3 MRI slices during intervention.

Compared to our previous work in phantoms [11], some changes were made to improve planning and navigation. Additional informational labels were added to the screen, highlighting the

patient's orientation. The entry and target points can now be positioned on separate slices of a 3D MRI dataset, allowing for greater flexibility in the selection of a needle trajectory. This may be useful in avoiding critical anatomic structures. Based on the needle trajectory, the MRI volume was resliced in three perpendicular planes that were displayed on the screen (Figure 5). This allowed visualization of the full path of the needle in two perpendicular slices. Usability was improved by adding zoom and pan features (Figure 3).

Workflow

The workflow we previously described in detail in our phantom study [11] was followed. We describe it briefly below. A pair of TipTAGs was attached to the needle hub and automatically calibrated when shown to the cameras of the optical head. Before obtaining each registration scan, the VisiMARKERs were placed around the area of intervention. At least 7 markers were placed around the target area for automatic segmentation and registration. The system requires a minimum of 4 markers to be visible to the optical head at any time for tracking. At each anatomic location, T1- and T2- weighted MRI volumetric scans were obtained for registration. The MRI registration scans were transferred from the MRI scanner to the planning console using a USB stick. The MRI bed was shifted out of the bore and the optical head was adjusted to capture the area of intervention. The system automatically segmented the T1-weighted MRI dataset and registered the fiducial markers to the optical head.

Two interventional radiologists who routinely perform image-guided needle biopsy, aspiration, and injection procedures participated in the study. They reviewed the images, selected the target and skin entry points, and planned the optimal needle path on the CORE computer. This path could be reviewed in multiple planes to ensure that no critical structures were located in the planned needle path. Each operator then inserted the calibrated needle at the skin entry point and followed the system-provided guidance until the needle reached the selected target, or a point close to the target that was satisfactory. For each insertion, the trajectory plan and final needle tip location was logged to the system for later evaluation. Finally, the confirmation scan was obtained with T1- and T2- weighted MRI.

Overall, each MRI scan took <2 minutes, and each insertion was completed within 1 minute to 3 minutes. The MRI-compatible needles that were used for all insertions were 10 cm in length. The needles used for shoulders, hips and SI joints were 20G and 22G needles commonly used for joint injections (Innovative Tomography Products GmbH). The liver "lesion" was targeted using a 18G Semi-Automatic Needle Biopsy Gun through a 16G coaxial needle introducer (Invivo, Schwerin, Germany). In total, the two interventional radiologists performed 12 needle insertions, including 3 in the shoulders, 4 in the hips, 4 in the SI joints, and one in the liver.

Data Analysis

Pre- and post-insertion MRI volumes were rigidly registered using common landmarks. Therefore, error estimates we provide in this work incorporate uncertainty due to soft tissue displacement from variability in pressure exerted by the MR imaging coil. 3D slicer [12] was used for manual landmark selection, registration, and segmentation of the needle tip.

The system reported 3 types of errors: user error, overall error, and system error. "User error" was the final distance between the system-calculated needle tip and selected target upon completion of insertion, as reported to the radiologist in real-time. "System error" was the distance between the manual needle tip segmentation and the tip location reported by the system. "Overall targeting error"

was calculated as the distance between the manually segmented needle tip and the chosen target location.

4. Results

The system did not cause any interruptions or imaging interference during the registration and confirmation scans when it was placed just outside of the 300 Gauss line. All procedures were completed without the need to turn the system on or off in the interventional MR suite. Overall, 12 locations were targeted, including 3 in the shoulders, 4 in the hips, 4 in the SI joints, and one in the liver, with the average insertion depth of 43±5 mm. An example of the procedure workflow for the left hip joint shows the planned selected target and skin entry points and planned needle trajectory before needle insertion on the left and the post-needle insertion scan to verify needle path and tip location on the right (Figure 6).

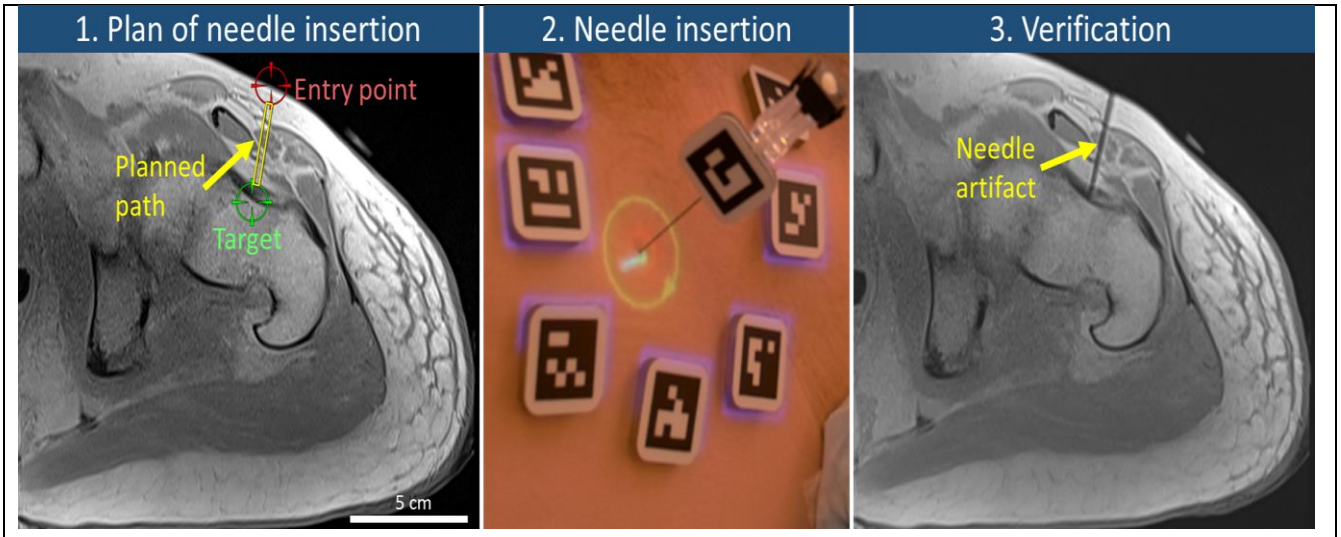

Figure 6. Needle insertion into the left hip joint was planned using a T1-weighted MRI dataset (Panel 1). The needle was then inserted by the radiologist with the help of system-projected guidance (Panel 2) until the target was reached. Needle position was verified, and error was quantified based on the needle artifact visible on a post-insertion T1-weighted scan (Panel 3).

The "user error" was 2.4±1.1 mm (range: 0.8 – 4.2 mm), "system error" was 2.2±0.8 mm (range 0.63 – 3.36 mm) and "overall targeting error" was 2.6±0.6 mm (range: 1.5 – 3.6 mm). Table 1 and Figure 7A illustrate the values for 3 types of errors and the depth of insertions for 12 targets.

Table 1. Summary of 3 types of error estimates and insertion depth based on 12 needle insertions.

Target	User error	System error	Overall targeting	Insertion depth	Needle gauge
Left shoulder 1	0.9	2.1	2.2	33.1	22
Left shoulder 2	3.0	2.7	3.2	43.2	22
Right shoulder 1	2.4	2.2	3.0	39.9	22
Left hip 1	3.6	3.4	2.4	42.0	22
Left hip 2	4.1	0.6	3.6	43.6	20
Right hip 1	1.5	3.2	3.4	53.1	22
Right hip 2	1.7	1.2	2.4	43.5	20
Liver	0.8	2.9	3.0	51.3	16
Left SI joint 1	3.4	3.3	2.2	46.0	20
Left SI joint 2	2.1	1.6	1.8	41.4	20
Right SI joint 1	4.2	2.3	2.4	35.7	22
Right SI joint 2	1.7	1.0	1.5	42.0	22

During each insertion, to minimize the pseudo shadow, the radiologist performed several actions, including advancing the needle, stopping, letting go of the needle, reorienting it, and/or pulling back. These actions are represented on a spaghetti plot in Figure 7B for insertions into shoulder, hip, SI joint, and liver.

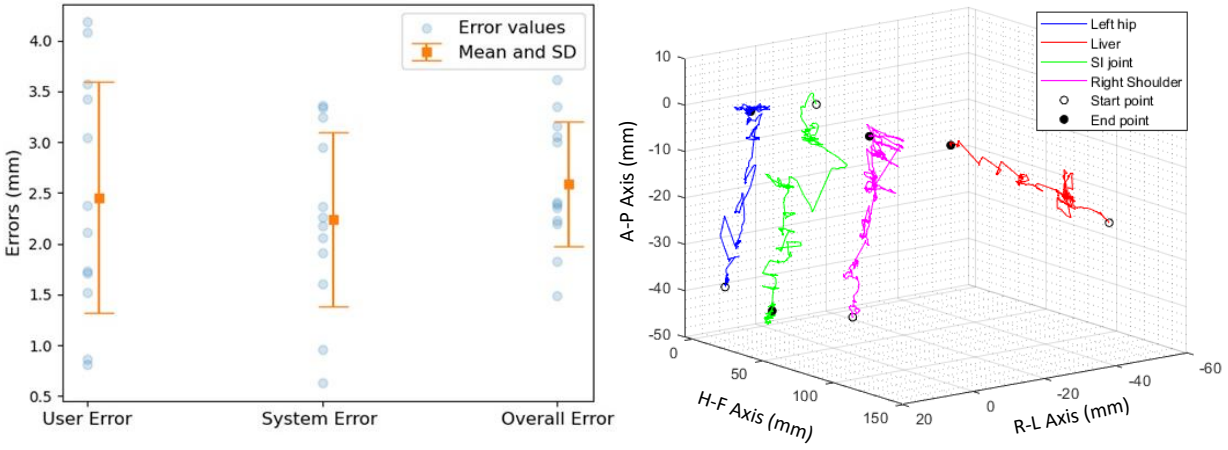

Figure 7. Error estimates and needle tip trajectory examples. A: Scatter plot of 3 error types for 12 needle insertions. B: Traces of needle tip location, as reported by the system, during image-guided needle insertions in four anatomic locations. The traces depict relative tip positions, as they have been shifted to ease visualization of several insertions.

5. Discussion

This work focused on evaluating and characterizing the feasibility and performance of needle placement under MRI-guidance in a human cadaver using an augmented reality system designed to enable MR-guided interventions. The cadaver experiments provide relevant human anatomical targets and conditions that are closer to the clinical setting in order to ensure that accuracy and operation of the AR-guidance system are sufficient to proceed to the clinical trial. User level of confidence and ease of use within the clinical workflow were qualitatively assessed.

Several features of the cadaver study are relevant for clinical translation. One of these is an ability to implement a workflow that would be directly applicable in the clinic. Second, tissue heterogeneity along the needle insertion path may result in deflection of the needle tip that is hard to anticipate in a homogeneous phantom. Since tissue characteristics of a cadaver are closer to those of a patient, the cadaver model provides more realistic tactile feedback to the radiologist. Another aspect of this study is that it provides a realistic assessment of needle visibility on MRI in and around clinically relevant targets. The experience provided herein as well as our previous work in phantoms show that needle insertion based on a planning scan is sufficient to achieve overall targeting error in the range of a few millimeters (1.5 – 3.6 mm). Thus, for this level of targeting accuracy, there may not be a need for intermediate scans ("advance and check" approach) during needle insertion. Lastly, while MR-compatible needles used here can be localized on MRI, additional insertions of larger bone biopsy needles, e.g. for bone biopsy, currently produce large imaging artifacts that completely obscured the actual needle. This makes localization of needle impossible on MRI, pointing to the need for a guidance system that does not rely on either the advance and check approach or post-insertion imaging.

The MRI-safe needles used in our study did not appear to bend during insertion. However, bending could be an issue for even thinner needles or deeper targets and stiffer tissues. The current technology has been designed to address rigid motion during the procedure automatically through optical tracking. There was no respiratory motion in this study, but since respiratory motion is a potential problem in the clinic, our team is working on incorporating motion compensation to address breathing motion for solid organ biopsy and treatment.

System-related limitations, some of which we previously identified, have been further examined in this work. A limitation is that sufficient space around the target area is needed for positioning the VisiMARKERs in a way that is not obstructed to the optical head. In this study, these markers were all placed on the skin, necessitating removal of the MRI imaging coil to ensure that enough markers were visible to the optical head during needle insertion. This can be addressed by using coils specifically designed for interventions that have larger openings and can remain in place during needle insertion, potentially reducing tissue displacement and improving accuracy and simplifying post-procedural analysis. The use of tip tags for needle tracking required that the needle is held and advanced in a way that does not obstruct the tag's visibility to the optical head. Needle length must also be sufficient to accommodate tag placement. To address this limitation, we have implemented a machine learning-based algorithm that enables needle tracking without the use of tip tags. Our ongoing clinical trial (NCT#06224933, https://classic.clinicaltrials.gov/ct2/show/NCT06224933) uses this improvement.

6. Conclusion

This study demonstrates that the performance of the LUMENA AR needle guidance system in a human cadaver is similar to that previously reported in phantoms. All needle insertions were successfully completed by two experienced interventional radiologists who routinely perform image-guided needle-based procedures. These operators relied only on the needle guidance that was projected onto the skin at/near the target area or on the planning console with no intermittent scans to ensure that the needle was following the correct planned trajectory. Additional improvements were made to this system prior to its clinical evaluation based on this work through an ongoing pilot clinical trial at our institution. This ongoing trial will evaluate clinical feasibility and safety of using the augmented reality needle guidance system during MR-guided procedures in pediatric and young adult patients.

7. Disclosures

Conflict of Interest

Drs. Rajan, Hossbach, Demir, and Foroughi are employees of Clear Guide Medical Inc., the manufacturers of the device being evaluated in this work. The other authors declare that they have no financial interests, commercial affiliations, or other potential conflicts of interest that could have influenced the objectivity of this research or the writing of this paper.

Data Availability Statement

The manuscript relies on data that have been fully included within the body of the manuscript.

Acknowledgements and Funding Sources

This work was supported by NIH grant 5R44EB028722.

Informed Consent:

This work does not involve human subjects and therefore formal consent was not required.

8. References

1. Floridi C, Cellina M, Irmici G, Bruno A, Rossini N, Borgheresi A, Agostini A, Bruno F, Arrigoni F, Arrichiello A, Candelari R, Barile A, Carrafiello G, Giovagnoni A. Precision Imaging Guidance in the Era of Precision Oncology: An Update of Imaging Tools for Interventional Procedures. Journal of Clinical Medicine. 2022;11(14):4028. PMID: doi:10.3390/jcm11144028.

2. Smith KA, Carrino JA. MRI-guided interventions of the musculoskeletal system. J Magn Reson Imaging. 2008;27(2):339-46. doi: 10.1002/jmri.21274. PMID: 18219687.

3. Bosch de Basea Gomez M, Thierry-Chef I, Harbron R, Hauptmann M, Byrnes G, Bernier M-O, Le Cornet L, Dabin J, Ferro G, Istad TS, Jahnen A, Lee C, Maccia C, Malchair F, Olerud H, Simon SL, Figuerola J, Peiro A, Engels H, Johansen C, Blettner M, Kaijser M, Kjaerheim K, Berrington de Gonzalez A, Journy N, Meulepas JM, Moissonnier M, Nordenskjold A, Pokora R, Ronckers C, Schüz J, Kesminiene A, Cardis E. Risk of hematological malignancies from CT radiation exposure in children, adolescents and young adults. Nature Medicine. 2023;29(12):3111-9. doi: 10.1038/s41591-023-02620-0.

4. Gao W, Jiang B, Kacher DF, Fetics B, Nevo E, Lee TC, Jayender J. Real-time probe tracking using EM-optical sensor for MRI-guided cryoablation. Int J Med Robot. 2018;14(1). Epub 20171128. doi: 10.1002/rcs.1871. PMID: 29193606.

5. Huang S, Lou C, Zhou Y, He Z, Jin X, Feng Y, Gao A, Yang G-Z. MRI-guided robot intervention—current state-of-the-art and new challenges. Med-X. 2023;1(1):4. doi: 10.1007/s44258-023-00003-1.

6. Cho J, Rahimpour S, Cutler A, Goodwin CR, Lad SP, Codd P. Enhancing Reality: A Systematic Review of Augmented Reality in Neuronavigation and Education. World Neurosurg. 2020;139:186-95. Epub 20200418. doi: 10.1016/j.wneu.2020.04.043. PMID: 32311561.

7. Acidi B, Ghallab M, Cotin S, Vibert E, Golse N. Augmented reality in liver surgery. J Visc Surg. 2023;160(2):118-26. Epub 20230213. doi: 10.1016/j.jviscsurg.2023.01.008. PMID: 36792394.

8. Fritz J, P UT, Ungi T, Flammang AJ, Cho NB, Fichtinger G, Iordachita, II, Carrino JA. Augmented reality visualization with image overlay for MRI-guided intervention: accuracy for lumbar spinal procedures with a 1.5-T MRI system. AJR Am J Roentgenol. 2012;198(3):W266-73. doi: 10.2214/AJR.11.6918. PMID: 22358024.

9. Mewes A, Heinrich F, Kagebein U, Hensen B, Wacker F, Hansen C. Projector-based augmented reality system for interventional visualization inside MRI scanners. Int J Med Robot. 2019;15(1):e1950. Epub 20180904. doi: 10.1002/rcs.1950. PMID: 30168639.

10. Li G, Patel NA, Melzer A, Sharma K, Iordachita I, Cleary K. MRI-guided lumbar spinal injections with body-mounted robotic system: cadaver studies. Minim Invasive Ther Allied Technol. 2022;31(2):297-305. Epub 20200730. doi: 10.1080/13645706.2020.1799017. PMID: 32729771.

11. Foroughi P, Demir A, Hossbach M, Rajan P, Yarmolenko P, Vellody R, Cleary K, Sharma K. In situ guidance for MRI interventions using projected feedback. Int J Comput Assist Radiol Surg. 2023;18(6):1069-76. Epub 20230418. doi: 10.1007/s11548-023-02897-z. PMID: 37072658.

12. Kikinis R, Pieper SD, Vosburgh KG. 3D Slicer: A Platform for Subject-Specific Image Analysis, Visualization, and Clinical Support. In: Jolesz FA, editor. Intraoperative Imaging and Image-Guided Therapy. New York, NY: Springer New York; 2014. p. 277-89.